

NOTES ON QUANTUM MAASS FORMS

ROELOF BRUGGEMAN

In my contribution to the proceedings¹ of the Fukuoka conference on L -series, I skipped some computations that may take some time to reproduce. For the record, I put these computations on my website, together with some additional comments.

References without primes are to the paper for the Fukuoka proceedings.

1.1'. **Twisted L -series for a Maass cusp form.** To check (8) in the contribution to the proceedings, I recall the twisted L -series for $u \in \text{Mf}_s^0$ with expansion (3). For $\xi \in \mathbb{Q}$ and $\text{Re } \rho$ sufficiently large:

$$\begin{aligned} L_e(\rho, \xi) &= \sum_{n \neq 0} a_n |n|^{-\rho} e^{2\pi i n \xi}, \\ L_o(\rho, \xi) &= \sum_{n \neq 0} n a_n |n|^{-\rho-1} e^{2\pi i n \xi}. \end{aligned} \quad (1')$$

Note that $L(\rho) = L_e(\rho, 0)$ for even u , and $L(\rho) = L_o(\rho, 0)$ for odd u . These L -functions are connected to the integrals

$$\begin{aligned} I(\rho, \xi) &= \int_0^\infty u(\xi + iy) y^{\rho - \frac{3}{2}} dy = \gamma_s(\rho) L_e(\rho, \xi), \\ J(\rho, \xi) &= \int_0^\infty \partial_x u(\xi + iy) y^{\rho - \frac{1}{2}} dy = 2\pi i \gamma_s(\rho + 1) L_o(\rho, \xi), \\ \gamma_s(\rho) &= \frac{\Gamma\left(\frac{\rho - s + \frac{1}{2}}{2}\right) \Gamma\left(\frac{\rho + s - \frac{1}{2}}{2}\right)}{4\pi^\rho}. \end{aligned} \quad (2')$$

The exponential decay at cusps of u and its derivatives implies that $I(\rho, \xi)$ and $J(\rho, \xi)$ are holomorphic in $\rho \in \mathbb{C}$. Hence L_e and L_o are also holomorphic in ρ , and have zeros to compensate for the singularities of γ_s . In particular:

$$L_e\left(s - \frac{1}{2}, \xi\right) = L_e\left(\frac{1}{2} - s, \xi\right) = 0 \quad \text{for all } \xi \in \mathbb{Q}. \quad (3')$$

For the functional equation we write $\xi = \frac{a}{c} = \gamma^\infty$ for some $\begin{bmatrix} a & b \\ c & d \end{bmatrix} \in \Gamma$ with $c > 0$. Put $\xi' = -\frac{d}{c} = \gamma^{-1}\infty$. The invariance of u gives

$$I(\rho, \xi) = \int_0^\infty u\left(\xi' + \frac{i}{c^2 y}\right) y^{\rho - \frac{3}{2}} dy = c^{1-2\rho} I(1 - \rho, \xi'). \quad (4')$$

¹p. 1–15 in *The conference on L-functions*, Fukuoka, Japan 18 - 23 February 2006, ed. Lin Weng & Masanobu Kaneko; World Scientific, 2007

For J we use that $\frac{\partial u}{\partial x} = \frac{\partial z}{\partial x} + \frac{\partial u}{\partial \bar{z}}$, $(-cz + a)^{-2} \frac{\partial u}{\partial \bar{z}}(\gamma^{-1}z) = \frac{\partial u}{\partial \bar{z}}(z)$, and similarly for $\frac{\partial u}{\partial \bar{z}}$.

$$\begin{aligned} J(\rho, \xi) &= - \int_0^\infty (yc)^{-2} \left(\frac{\partial u}{\partial z} \left(\xi' + \frac{i}{c^2 y} \right) + \frac{\partial u}{\partial \bar{z}} \left(\xi' + \frac{i}{c^2 y} \right) \right) y^{\rho+\frac{1}{2}} \frac{dy}{y} \\ &= -c^{1-2\rho} J(1-\rho, \xi'). \end{aligned} \quad (5')$$

Thus, we have the functional equations

$$\begin{aligned} \gamma_s(\rho) L_e(\rho, \xi) &= c^{1-2\rho} \gamma_s(1-\rho) L_e(1-\rho, \xi'), \\ \gamma_s(\rho+1) L_o(\rho, \xi) &= -c^{1-2\rho} \gamma_s(2-\rho) L_o(1-\rho, \xi'). \end{aligned} \quad (6')$$

After recalling these well known facts, we turn to the method in §4, Chap. I of [3]. Let f be the periodic function in (4), which takes for general u the following form:

$$f(\tau) = \frac{1}{2} \pi^s \Gamma(1-s) \text{sign}(\text{Im } \tau) \sum_{n \mid \text{Im } \tau > 0} |n|^{s-\frac{1}{2}} a_n e^{2\pi i n \tau}. \quad (7')$$

The Mellin transform of $y \mapsto f(\xi \pm iy)$ is

$$\tilde{f}_\pm(\rho, \xi) = 2^{-\rho-2} \pi^{s-\rho} \Gamma(1-s) \Gamma(\rho) \left(\pm L_e \left(\rho + \frac{1}{2} - s, \xi \right) + L_o \left(\rho + \frac{1}{2} - s, \xi \right) \right). \quad (8')$$

The L -functions have polynomial decay on vertical strips. So we can transform the Mellin representation of $f(\xi \pm iy)$ into

$$f(\xi \pm iy) = \frac{1}{2\pi i} \int_{\text{Re } \rho = -\varepsilon} \tilde{f}_\pm(\rho, \xi) y^{-\rho} d\rho + \text{Res}_{\rho=0} \tilde{f}_\pm(\rho, \xi), \quad (9')$$

with some small $\varepsilon > 0$. The integral contributes $o(1)$ as $y \downarrow 0$. So the limit value is

$$f(\xi) = \frac{\pi^s}{4} \Gamma(1-s) L_o \left(\frac{1}{2} - s, \xi \right) = -\frac{c^{2s}}{4\pi^{s+\frac{1}{2}}} \Gamma \left(s + \frac{1}{2} \right) L_o \left(s + \frac{1}{2}, \xi' \right). \quad (10')$$

As in [3], one can show that (9') is valid for general $\tau \in \mathfrak{H} \cup \mathfrak{H}^-$. This gives the same limit valid under geodesic approach.

1.2'. **Eisenstein series.** To obtain (16), we first consider

$$h_s(\tau) = \sum_{n=1}^{\infty} \sigma_{2s-1}(n) e^{\pm 2\pi i n \tau} \quad (11')$$

with the convention $\pm 1 = \text{sign}(\text{Im } \tau)$. So f_s in (15) is given by

$$f_s(\tau) = \pm \frac{\sqrt{\pi} \Gamma(1-s) \Lambda(2s)}{2\Gamma\left(\frac{1}{2}-s\right)} \pm \pi^s \Gamma(1-s) h_s(\tau). \quad (12')$$

Let $\xi = \gamma_\infty = \frac{a}{c}$ as before. The Mellin transform of $y \mapsto h_s(\xi \pm iy)$ is

$$\begin{aligned} \tilde{m}_\pm(\rho, \xi) &= \sum_{n=1}^{\infty} \sigma_{2s-1}(n) e^{\pm 2\pi i n \xi} (2\pi n)^{-\rho} \Gamma(\rho) \\ &= (2\pi)^{-\rho} \Gamma(\rho) c^{2s-1-2\rho} \sum_{1 \leq x, y \leq c} e^{\pm 2\pi i xy a/c} \zeta \left(\rho + 1 - 2s, \frac{x}{c} \right) \zeta \left(\rho, \frac{y}{c} \right), \end{aligned} \quad (13')$$

with the Hurwitz zeta function, see e.g., §1, Chap. XIV of S.LANG: *Introduction to modular forms*; Springer-Verlag, 1976.

Like for a cusp form, we obtain a Mellin representation that implies

$$h_s(\xi + w) = \sum_r (\mp iw)^{-r} \operatorname{Res}_{\rho=r} \tilde{m}_{\pm}(\rho, \xi) + o(1) \quad w \xrightarrow{\text{ga}} 0, \quad (14')$$

where r runs over the residues in the region $\operatorname{Re} \rho \geq 0$. The residue at $\rho = 1$ is

$$\begin{aligned} (2\pi)^{-1} c^{2s-3} \sum_{x=1}^c \zeta\left(2-2s, \frac{x}{c}\right) \sum_{y=1}^{c-1} e^{\pm 2\pi i x y a/c} \\ = (2\pi)^{-1} c^{2s-2} \zeta(2-2s). \end{aligned} \quad (15')$$

At $\rho = 2s$:

$$\begin{aligned} (2\pi)^{-2s} \Gamma(2s) c^{-2s-1} \sum_{y=1}^c \zeta\left(2s, \frac{y}{c}\right) \sum_{x=1}^c e^{\pm 2\pi i x y a/c} \\ = (2\pi)^{-2s} \Gamma(2s) c^{-2s} \zeta(2s). \end{aligned} \quad (16')$$

The residue at $\rho = 0$ is more complicated. With $\zeta(0, a) = \frac{1}{2} - a$:

$$\begin{aligned} c^{2s-1} \sum_{1 \leq x, y \leq c} e^{\pm 2\pi i x y a/c} \zeta\left(1-2s, \frac{x}{c}\right) \left(\frac{1}{2} - \frac{y}{c}\right) \\ = -\frac{1}{2} c^{2s-1} \sum_{x=1}^c \zeta\left(1-2s, \frac{x}{c}\right) \\ - c^{2s-1} \sum_{y=1}^{c-1} \left(\left(\frac{y}{c}\right)\right) \sum_{x=1}^c e^{\pm 2\pi i x y a/c} \zeta\left(1-2s, \frac{x}{c}\right), \end{aligned} \quad (17')$$

where $((x)) = x - \frac{1}{2}$ if $0 < x < 1$, $((0)) = 0$, and $((x+n)) = ((x))$ for $n \in \mathbb{Z}$.

The former term in (17') is $-\frac{1}{2} \zeta(1-2s)$. The latter term equals

$$-c^{2s-1} \sum_{y=1}^{c-1} \left(\left(\frac{dy}{c}\right)\right) \sum_{x=1}^c e^{\pm 2\pi i x y/c} \zeta\left(1-2s, \frac{x}{c}\right), \quad (18')$$

which is meromorphic in s . For large s we have

$$\begin{aligned} \sum_{x=1}^c e^{\pm 2\pi i x y/c} \zeta\left(1-2s, \frac{x}{c}\right) \\ = \sum_{x=1}^c e^{\pm 2\pi i x y/c} (-i) (2\pi)^{-2s} \Gamma(2s) \sum_{n \geq 1} n^{-2s} \left(e^{2\pi i n x/c + \pi i (\frac{1}{2}-s)} - e^{-2\pi i n x/c - \pi i (\frac{1}{2}-s)} \right) \\ = (2\pi)^{-2s} \Gamma(2s) c \left(e^{-\pi i s} \sum_{n \geq 1, n \equiv \mp y(c)} n^{-2s} + e^{\pi i s} \sum_{n \geq 1, n \equiv \pm y(c)} n^{-2s} \right) \end{aligned}$$

$$= (2\pi)^{-2s} \Gamma(2s) c^{1-2s} \left(\zeta\left(2s, \frac{c-y}{c}\right) e^{\mp\pi is} + \zeta\left(2s, \frac{y}{c}\right) e^{\pm\pi is} \right).$$

This relation stays valid under meromorphic continuation. We insert it into (18'):

$$\begin{aligned} & -(2\pi)^{-2s} \pi^{-\frac{1}{2}} 2^{2s-1} \Gamma(s) \Gamma\left(s + \frac{1}{2}\right) \\ & \quad \cdot \sum_{y=1}^{c-1} \left(\left(\frac{dy}{c} \right) \right) \left(\zeta\left(2s, 1 - \frac{c}{y}\right) e^{\mp\pi is} + \zeta\left(2s, \frac{y}{c}\right) e^{\pm\pi is} \right) \\ & = -\frac{1}{2} \pi^{-2s-\frac{1}{2}} \Gamma(s) \Gamma\left(s + \frac{1}{2}\right) \sum_{y=1}^{c-1} \left(\left(\frac{dy}{c} \right) \right) \zeta\left(2s, \frac{y}{c}\right) (-e^{\mp\pi is} + e^{\pm\pi is}) \\ & = \mp i \pi^{\frac{1}{2}-2s} \frac{\Gamma\left(s + \frac{1}{2}\right)}{\Gamma(1-s)} \sum_{y=1}^{c-1} \left(\left(\frac{dy}{c} \right) \right) \zeta\left(2s, \frac{y}{c}\right). \end{aligned} \quad (19')$$

Thus we obtain expansions of h_s and f_s , as $w \xrightarrow{\text{ga}} 0$:

$$\begin{aligned} h_s(\xi + w) &= (2\pi)^{-1} c^{2s-2} \zeta(2-2s) (\mp iw)^{-1} + (2\pi)^{-2s} c^{-2s} \Gamma(2s) \zeta(2s) (\mp iw)^{-2s} \\ & \quad - \frac{1}{2} \zeta(1-2s) \mp i \pi^{\frac{1}{2}-2s} \frac{\Gamma\left(s + \frac{1}{2}\right)}{\Gamma(1-s)} \sum_{y=1}^{c-1} \left(\left(\frac{dy}{c} \right) \right) \zeta\left(2s, \frac{y}{c}\right) o(1), \end{aligned} \quad (20')$$

$$\begin{aligned} f_s(\xi + w) &= \frac{i}{2} c^{2s-2} \Lambda(2s-1) \frac{1}{w} \pm \frac{1}{2\sqrt{\pi}} c^{-2s} \Gamma(1-s) \Gamma\left(s + \frac{1}{2}\right) \Lambda(2s) (\mp iw)^{-2s} \\ & \quad - i \pi^{\frac{1}{2}-s} \Gamma\left(s + \frac{1}{2}\right) \sum_{y=1}^{c-1} \left(\left(\frac{dy}{c} \right) \right) \zeta\left(2s, \frac{y}{c}\right) + o(1). \end{aligned} \quad (21')$$

Invariance. In §1.2.2 it is noted that the middle term in (16) determines a Γ -invariant element of $\tilde{\mathcal{H}}_s$. Up to a factor, the middle term is given by

$$m\left(\frac{a}{c}, \frac{a}{c} + w\right) = \pm |c|^{-2s} (\mp iw)^{-2s} + o(1) \quad (w \xrightarrow{\text{ga}} 0), \quad (22')$$

for $\frac{a}{c} \in \mathbb{Q}$, where we assume $a, c \in \mathbb{Z}$, $(a, c) = 1$. To get the equality $m = m|_{2s}\gamma$ in $\tilde{\mathcal{H}}_s$, we need to check it at almost all rational points for a system of generators of Γ . Let us use the standard generators $T = \begin{bmatrix} 1 & 1 \\ 0 & 1 \end{bmatrix}$ and $S = \begin{bmatrix} 0 & -1 \\ 1 & 0 \end{bmatrix}$. For T the invariance is obvious. For S we work with $\frac{a}{c} \neq 0$.

$$\begin{aligned} (m|_{2s}S)\left(\frac{a}{c}, \frac{a}{c} + w\right) &= \left(\left(\frac{a}{c} + w\right)^2\right)^{-s} m\left(-\frac{c}{a}, \frac{-1}{\frac{a}{c} + w}\right) \\ &= \left|\frac{a}{c}\right|^{-2s} \left(1 + \frac{cw}{a}\right)^{-2s} (\pm 1) |a|^{-2s} \left(\mp i \left(\frac{-1}{\frac{a}{c} + w} + \frac{c}{a}\right)\right)^{-2s} + o(1) \\ &= \pm |c|^{2s} |a|^{-4s} \left(1 + \frac{cw}{a}\right)^{-2s} \left(\mp i \left(\frac{c}{a}\right)^2 \frac{w}{1 + \frac{cw}{a}}\right)^{-2s} + o(1) \end{aligned} \quad (23')$$

$$= \pm |c|^{-2s} (\mp iw)^{-2s} + o(1) = m \left(\frac{a}{c}, \frac{a}{c} + w \right). \quad (24')$$

2.2'. **Proof of Theorem 2.** It may be useful to add some more explanations. The idea is that the given invariant hyperfunction $\alpha \in (\mathcal{Y}_s^{-\omega})^\Gamma$ is written as

$$\alpha = \alpha^c + \alpha^0 + \alpha^{\infty,1} + \alpha^{\infty,2}, \quad (25')$$

corresponding to parts of the Fourier expansion 21:

$$\begin{aligned} \Pi_s \alpha^c(z) &= \sum_{n \neq 0} a_n \sqrt{|y|} K_{s-1/2}(4\pi|n|y) e^{2\pi i n x}, \\ \Pi_s \alpha^0(z) &= a_0 y^s, \\ \Pi_s \alpha^{\infty,1}(z) &= b_0 y^{1-s}, \\ \Pi_s \alpha^{\infty,2}(z) &= \sum_{n \neq 0} b_n \sqrt{|y|} I_{1/2-s}(4\pi|n|y) e^{2\pi i n x}. \end{aligned} \quad (26')$$

$$(27')$$

In the paper $\alpha^{\infty,1} + \alpha^{\infty,2}$ is called α^∞ .

2.2.1'. *Cuspidal part.* Let

$$f_u^c(\tau) = \pm \frac{\pi^s}{2} \Gamma(1-s) \sum_{n=1}^{\infty} n^{s-\frac{1}{2}} a_{\pm n} e^{\pm 2\pi i n \tau} \quad (28')$$

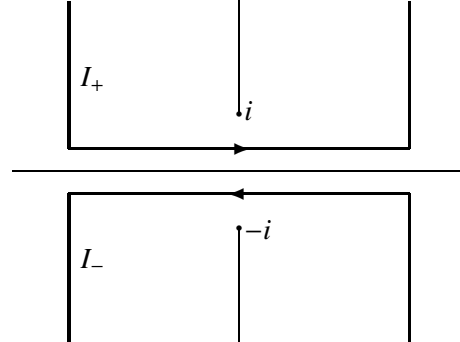
be the ‘‘cuspidal part’’ of the periodic holomorphic function f_u in (22). The proof of Lemma 4.2 in [1] gives a representative g_α^c of α^c by the integral

$$g_\alpha^c(\tau_0) = \frac{1}{2\pi i} \int_{I_+ \cup I_-} \frac{1 + \tau \tau_0}{\tau - \tau_0} f_u^c(\tau) (1 + \tau^2)^{s-1} d\tau, \quad (29')$$

with contours as sketched. The contours are adapted to τ_0 , such that τ_0 is in the region inside I_+ or inside I_- .

In the comparison with [1] one should use $\nu_{\text{there}} = s_{\text{here}} - \frac{1}{2}$.

One can check from the integral that g_α^c extends smoothly through a given geodesic through ∞ with value 0 at ∞ . Hence $g_\alpha^c(\tau_0) = o(1)$ as $\tau_0 \xrightarrow{\text{ga}} \infty$.



If we use the integral in (29') with τ_0 between I_+ and I_- , we define η holomorphic on a neighborhood of \mathbb{R} . So $\eta \in \mathcal{Y}_s^{\omega, \text{fs}}$. One can check that η has a smooth extension through ∞ along \mathbb{R} . So $\eta \in \mathcal{Y}_s^{\omega, \infty}$. Moving the contour across τ_0 , we arrive at $g_\alpha^c(\tau) = \eta(\tau) + (1 + \tau^2)^s f_u^c(\tau)$ for τ near \mathbb{R} .

Side remark. Let us for a moment suppose that $u \in \text{Mf}_s^0$. We have seen that $g_\alpha^c(\infty) = 0$. Now $\alpha = \alpha^c$ and g_α^c represents α . The Γ -invariance implies that $g_\alpha^c - g_\alpha^c|_{2s}^{\text{pr}} \gamma = r_\gamma \in \mathcal{Y}_s^\omega$. So $g_\alpha^c(\xi)$ is well defined for all $\xi \in \mathbb{Q}$, and thus we have a representative of $\mathfrak{q}_s^\omega u \in \mathfrak{qMf}_s^\omega$. The image $\mathfrak{q}_s^{\omega, \infty} u$ of $\mathfrak{q}_s^\omega u$ under the natural map

$\mathfrak{qMf}_s^\omega \rightarrow \mathfrak{qMf}_s^{\omega, \infty}$ can be represented by $\xi \mapsto g_\alpha^c(\xi) - \eta(\xi) = (1 + \xi^2)^s f_\alpha^c(\xi)$. That is the representative constructed in Theorem 1.

2.2.2'. *Constant terms in the Fourier expansion.* The hyperfunctions α^0 and $\alpha^{\infty, 1}$ have been discussed in [1]. Representatives on a neighborhood of ∞ are all we need, and are available in [1]. Note that the hyperfunction $\alpha^{\infty, 1}$ has support $\{\infty\}$ (if $b_0 \neq 0$).

2.2.3'. *Hyperfunction for the exponentially increasing terms.* The description of the remaining terms in the Fourier expansion goes along the same lines as in [1], but is not explicitly treated there. Here I give the computations underlying (23).

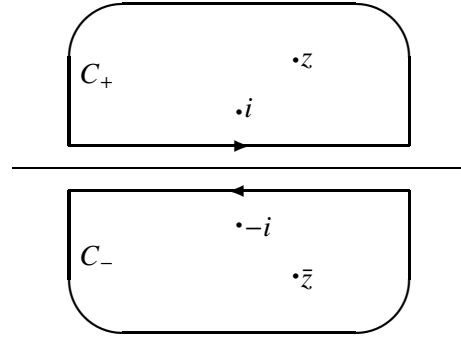
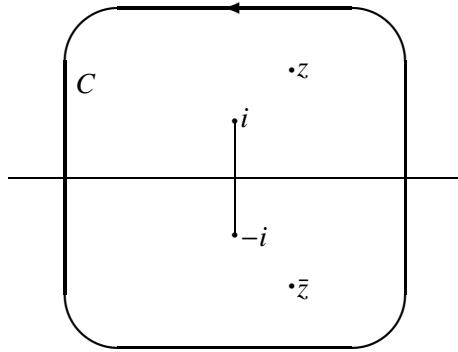
The convergence of (21) implies $b_n = O(e^{-A|n|})$ as $|n| \rightarrow \infty$ for each $A \in \mathbb{R}$. Since ${}_1F_1(1; a : u) \ll e^{\operatorname{Re} u} |u|^{\operatorname{Re} a} + 1$, the series in (23) converges absolutely and defines $g_\alpha^{\infty, 2}$ as a holomorphic function on $\mathbb{C} \setminus i[-1, 1]$. It represents a hyperfunction on $\mathbb{P}_{\mathbb{R}}^1 \setminus \{0\}$ with support contained in $\{\infty\}$. We extend it to $\mathbb{P}_{\mathbb{R}}^1$ by taking 0 on \mathbb{R} . Now our task is to check that (27') holds.

In the projective model, the Poisson integral is given by

$$\Pi_s \alpha^{\infty, 2}(z) = \frac{1}{\pi} \int_{C_+ \cup C_-} g(\tau) \left(\frac{y(1 + \tau^2)}{(\tau - z)(\tau - \bar{z})} \right)^{1-s} \frac{d\tau}{1 + \tau^2} \quad (30')$$

with contours as sketched, and g any global representative of $\alpha^{\infty, 2}$.

Since such a global representative is holomorphic on a neighborhood of \mathbb{R} , we can replace $C_+ \cup C_-$ by a wide contour C , around z , \bar{z} and the interval $i[-1, 1]$.



In the integral over C , we use that $g - g_\alpha^{\infty, 2}$ is holomorphic on a full neighborhood of ∞ , including $\infty \in \mathbb{P}_{\mathbb{R}}^1$. So we can replace g by $g_\alpha^{\infty, 2}$.

With the absolute convergence of (23) on compact sets, we arrive at the following integral representation:

$$\Pi_s \alpha^{\infty, 2}(z) = \frac{1}{\pi} \int_C g_\alpha^{\infty, 2}(\tau) \left(\frac{y(1 + \tau^2)}{(\tau - z)(\tau - \bar{z})} \right)^{1-s} \frac{d\tau}{1 + \tau^2}. \quad (31')$$

If C is sufficiently wide, we can replace C by $C + x$:

$$= \frac{-i\pi^{-\frac{1}{2}-s}}{2\Gamma\left(\frac{3}{2}-s\right)} \sum_{n \neq 0} |n|^{\frac{1}{2}-s} b_n y^{1-s} \int_C \left(1 + \frac{y^2}{\tau^2}\right)^{s-1} \left(1 + \frac{x}{\tau}\right)^{1-2s} \cdot {}_1F_1(1; 2-2s; 2\pi i n(\tau+x)) \frac{d\tau}{\tau}. \quad (32')$$

We use the absolute convergence of the series for ${}_1F_1$ and $(1+z)^a$ on compact sets, to find for the integral in (32')

$$\begin{aligned} &= \sum_{m \geq 0} \frac{(2\pi i n)^m}{(2-2s)_m} \int_C \left(1 + \frac{y^2}{\tau^2}\right)^{s-1} \left(1 + \frac{x}{\tau}\right)^{1-2s+m} \tau^{m-1} d\tau \\ &= \sum_{m \geq 0} \frac{(2\pi i n)^m}{(2-2s)_m} \sum_{a, b \geq 0} \binom{s-1}{a} \binom{2-2s+m}{b} y^{2a} x^b \int_C \tau^{-2a-b+m-1} d\tau \\ &= \sum_{a, b \geq 0} \frac{\Gamma(2-2s)\Gamma(s)\Gamma(2-2s+2a+b)}{\Gamma(2-2s+2a-b)\Gamma(s-a)\Gamma(2-2s+2a)} \frac{(2\pi i n)^{2a+b} y^{2a} x^b}{a! b!} 2\pi i \\ &= 2\pi i \sum_{a, b \geq 0} \frac{\pi^{-1/2} 2^{1-2s} \Gamma(1-s) \Gamma\left(\frac{3}{2}-s\right) \Gamma(s)}{\Gamma(s-a) \pi^{-1/2} 2^{1-2s+2a} \Gamma(1-s+a) \Gamma\left(\frac{3}{2}-s+a\right)} \\ &\quad \cdot \frac{(-1)^a (2\pi |n| y)^{2a} (2\pi i n x)^b}{a! b!} \\ &= 2\pi i \Gamma\left(\frac{3}{2}-s\right) \sum_{a \geq 0} \frac{(2\pi |n| y)^{2a}}{a! \Gamma\left(\frac{3}{2}-s+a\right)} \sum_{b \geq 0} \frac{(2\pi i n x)^b}{b!} \\ &= 2i\pi^{s+\frac{1}{2}} |n|^{s-\frac{1}{2}} y^{s-\frac{1}{2}} \Gamma\left(\frac{3}{2}-s\right) I_{1/2-s}(2\pi |n| y) e^{2\pi i n x}. \end{aligned}$$

With (31') and (32') we arrive at (27').

This computation only provides a confirmation of (27'). One can arrive at $\tau(1+\tau^{-2})^s {}_1F_1(1; 2-2s; 2\pi i n \tau)$ in (23) by solving

$$\frac{d}{dx} \beta \Big|_{2s}^{\text{pr}} \begin{bmatrix} t & x \\ 0 & 1 \end{bmatrix} \Big|_{x=0} = 2\pi i n \beta \quad (33')$$

with a hyperfunction β with support equal to $\{\infty\}$.

2.2.4'. *T-invariance.* In the proof of Theorem 2 we also need that B in (23) satisfies $B|_{2s}^{\text{pr}}(T-1)(\tau) = o(1)$ as $\tau \xrightarrow{\text{ga}} \infty$. Actually, we shall show this modulo a term τ^{-1} (Anal), where (Anal) denotes a holomorphic function on a neighborhood of ∞ . The estimate of b_n implies absolute convergence, and we can restrict our attention to one value of $n \neq 0$ at the time.

$$\begin{aligned} B_{2s}^{\text{pr}} T(\tau) - B(\tau) &= \left(\frac{1+\tau^2}{1+(\tau+1)^2}\right)^s (\tau+1) (1+(\tau+1)^{-2})^s \\ &\quad \cdot {}_1F_1(1; 2-2s; 2\pi i n(\tau+1)) - (1+\tau^{-2})^s {}_1F_1(1; 2-2s; 2\pi i n \tau) \end{aligned}$$

$$\begin{aligned}
&= (1 + \tau^{-2})^s \sum_{m=0}^{\infty} \frac{(2\pi i n)^m}{(2-2s)_m} \tau^{1+m} \left(\left(1 + \frac{1}{\tau}\right)^{1-2s+m} - 1 \right) \\
&= (\text{Anal}) \sum_{\substack{m \geq 0, k \geq 0 \\ 1+m-k \geq 0}} \frac{\Gamma(2-2s)(2\pi i n)^m \Gamma(2-2s+m)}{\Gamma(2-2s+m) k! \Gamma(2-2s+m-k)} \tau^{1+m-k} \\
&\quad + \tau^{-1} (\text{Anal}) \\
&= (\text{Anal}) \sum_{l \geq 0} \frac{(2\pi i n)^{l-1} \tau^l}{\Gamma(1-2s+l)} \sum_{k=1}^{\infty} \frac{(2\pi i n)^k}{k!} + \tau^{-1} (\text{Anal}) \\
&= (\text{Anal}) \sum_{l \geq 0} \frac{(2\pi i n)^{l-1} \tau^l}{\Gamma(1-2s+l)} (e^{2\pi i n} - 1) + \tau^{-1} (\text{Anal}) = \tau^{-1} (\text{Anal}) .
\end{aligned}$$

2.3'. One-sided average.

2.3.1'. *Hurwitz zeta function.* I think it is illuminating to recall the asymptotic behavior as $\tau \xrightarrow{\text{ga}} \infty$ of the Hurwitz zeta function $\zeta(u, \tau)$.

For $\text{Re } u > 1$, the series representation $\zeta(u, \tau) = \sum_{n=0}^{\infty} \tau^{-n-u}$ converges absolutely, and defines $u \mapsto \zeta(u, \tau)$ as a holomorphic function estimated by

$$\begin{aligned}
|\zeta(u, \tau)| &\leq \sum_{n=0}^{\infty} \left((\text{Im } \tau)^2 + (n + \text{Re } \tau)^2 \right)^{-\text{Re } u/2} e^{\pi |\text{Im } u|} \quad (34') \\
&\ll_u \int_{-\infty}^{\infty} \left(|\text{Im } \tau|^2 + v^2 \right)^{-\text{Re } u/2} dv \ll_{\text{Re } u} |\text{Im } \tau|^{1-\text{Re } u} .
\end{aligned}$$

Furthermore,

$$\begin{aligned}
\zeta(u, \tau) - \frac{\tau^{1-u}}{u-1} &= \sum_{n=0}^{\infty} \int_n^{n+1} \left((\tau+n)^{-u} - (\tau+v)^{-u} \right) du \quad (35') \\
&= \sum_{n=0}^{\infty} \int_n^{n+1} \left(\frac{u(v-n)}{\tau+n} + h_2(\tau, u, v-n) \right) dv ,
\end{aligned}$$

with $h_2(\tau, u, x)$ holomorphic in $u \in \mathbb{C}$ and $|h_2(\tau, u, x)| \leq C_u \frac{|v-n|^2}{|\tau+n|^2}$. So

$$\zeta(u, \tau) - \frac{\tau^{1-u}}{u-1} = \frac{u}{2} \zeta(u+1, \tau) + H_2(\tau, u), \quad (36')$$

with $H_2(\tau, u)$ holomorphic on $\text{Re } u > 0$ and

$$|H_2(\tau, u)| \ll_u \sum_{n=0}^{\infty} |\tau+n|^{-\text{Re } u-2} \ll_{\text{Re } u} |\text{Im } \tau|^{-\text{Re } u-1} . \quad (37')$$

So $\zeta(u, \tau)$ has a meromorphic continuation at least to $\text{Re } u > 0$, with a singularity only at $u = 1$, and as $\tau \xrightarrow{\text{ga}} \infty$:

$$\zeta(u, \tau) = \frac{\tau^{1-u}}{u-1} + \frac{u}{2} \zeta(u+1, \tau) + O_u \left(|\tau|^{-\text{Re } u-1} \right) \quad (38')$$

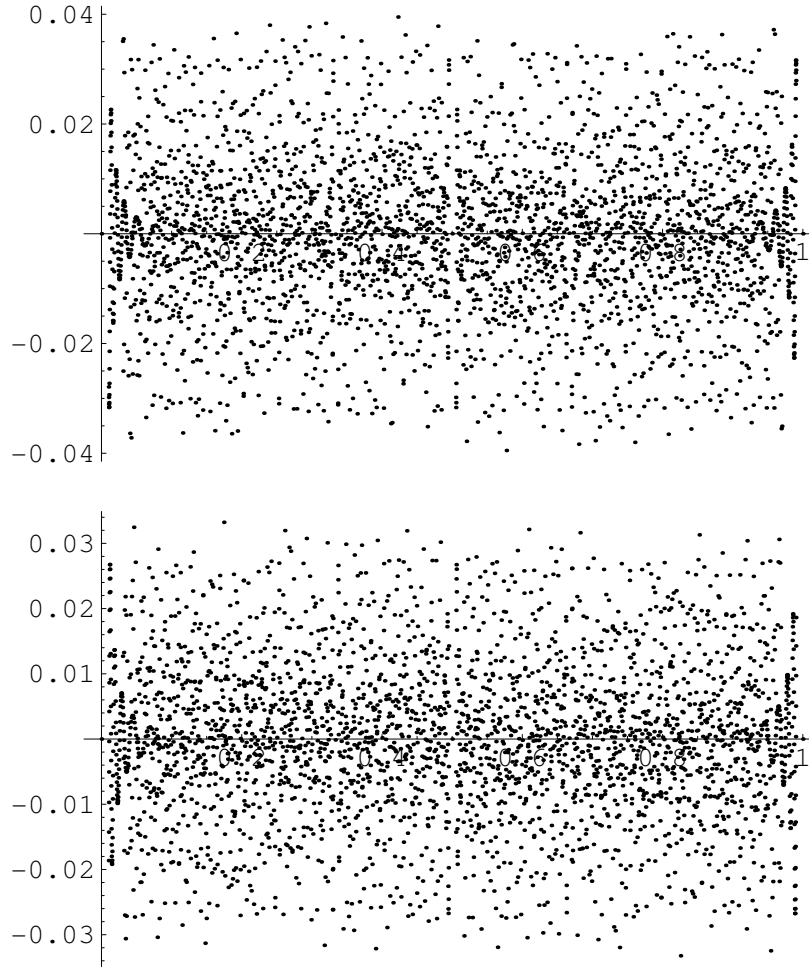


FIGURE 1. The quantum Maass form for the Eisenstein series E_{s_1} , with $\zeta(2s_1 - 1) = 0$, $2s_1 - 1 \approx \frac{1}{2} + 14.1347i$. Drawn are real part (top) and imaginary part (bottom) of $C_{s_1}(a/c)$ for $0 \leq \frac{a}{c} \leq 1$, $1 \leq c \leq 100$.

$$\begin{aligned}
 &= \frac{\tau^{1-u}}{u-1} + \frac{u}{2} \left(\frac{\tau^{-u}}{u} + \frac{u+1}{2} \zeta(u+2, \tau) + O_u(|\tau|^{-\operatorname{Re} u - 2}) \right) + o(1) \\
 &= \frac{\tau^{1-u}}{u-1} + \frac{\tau^{-u}}{2} + O_u(|\tau|^{-\operatorname{Re} u - 1}) + o(1) = \frac{\tau^{1-u}}{u-1} + \frac{\tau^{-u}}{2} + o(1).
 \end{aligned}$$

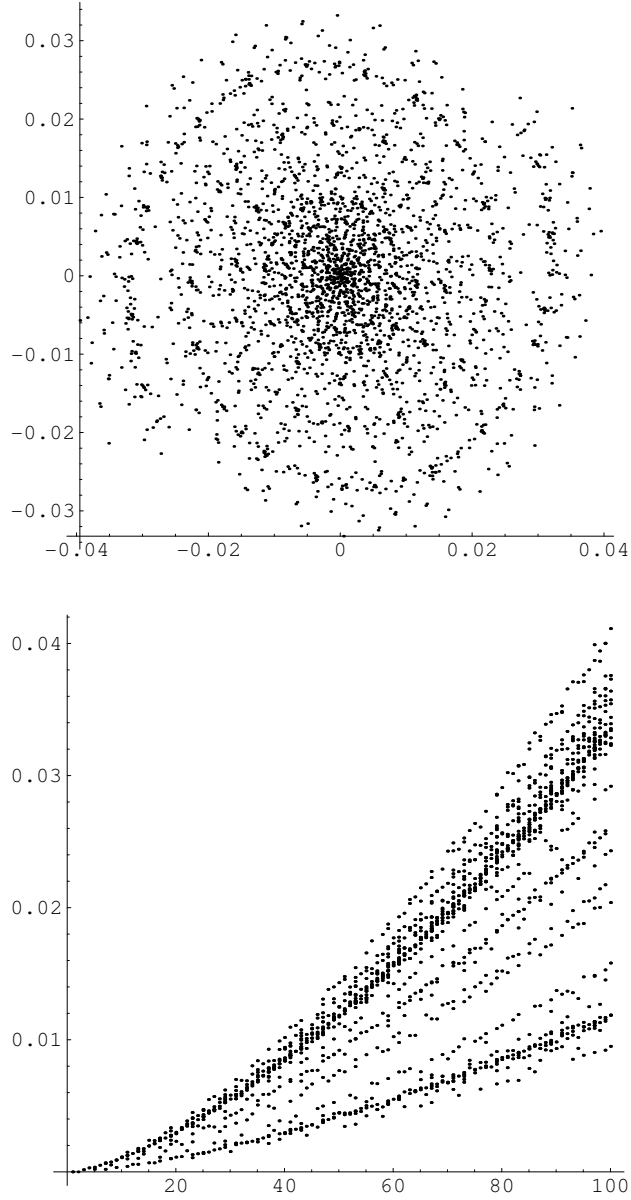


FIGURE 2. The quantum Maass form for the Eisenstein series E_{s_1} , with $\zeta(2s_1 - 1) = 0$, $2s_1 - 1 \approx \frac{1}{2} + 14.1347i$. In the top graph, the values of $C_{s_1}(a/c)$ are plotted in the complex plane, for $0 \leq \frac{a}{c} \leq 1$, $1 \leq c \leq 100$. The bottom graph gives $|C_{s_1}(a/c)|$ against the denominator c .

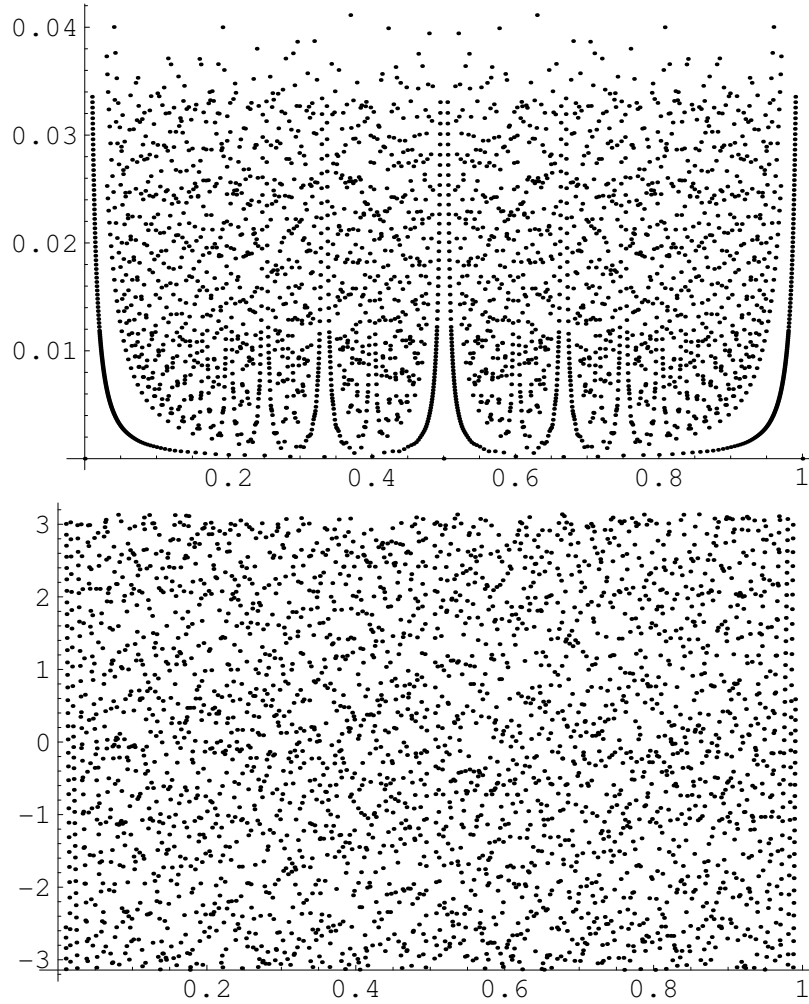


FIGURE 3. The quantum Maass form for the Eisenstein series E_{s_1} , with $\zeta(2s_1 - 1) = 0$, $2s_1 - 1 \approx \frac{1}{2} + 14.1347i$. Drawn are absolute value (top) and argument (bottom) of $C_{s_1}(a/c)$ for $0 \leq \frac{a}{c} \leq 1$, $1 \leq c \leq 100$.

2.3.2'. *One-sided average.* We apply this to the one-sided average of $f_0(\tau) = (1 + \tau^{-2})^s$. For $\text{Re } s > \frac{1}{2}$:

$$\begin{aligned}
 f_0|_{2s}^{\text{pr}} \text{Av}_T^+(\tau) &= \sum_{n=0}^{\infty} \left(\frac{1 + \tau^2}{1 + (\tau + n)^2} \right)^s (1 + (\tau + n)^{-2})^s \\
 &= \sum_{n=0}^{\infty} (1 + \tau^{-2})^s (1 + (\tau + n)^{-2})^{-s+s} \tau^{2s} (n + \tau)^{-2s}
 \end{aligned} \tag{39'}$$

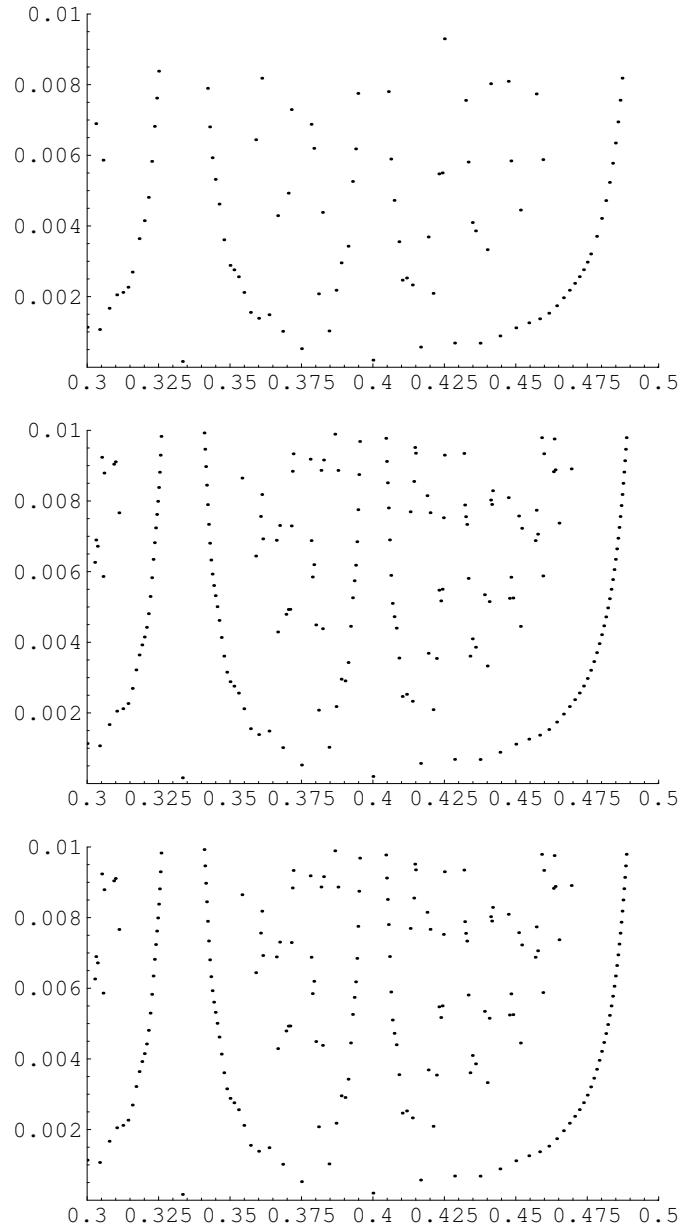


FIGURE 4. The quantum Maass form for the Eisenstein series E_{s_1} . Drawn is $|C_{s_1}(a/c)| \leq$ for $0.3 \leq \frac{a}{c} \leq 0.5$, $1 \leq c \leq N$, with $N = 40$, 100, and 140 (from top to bottom).

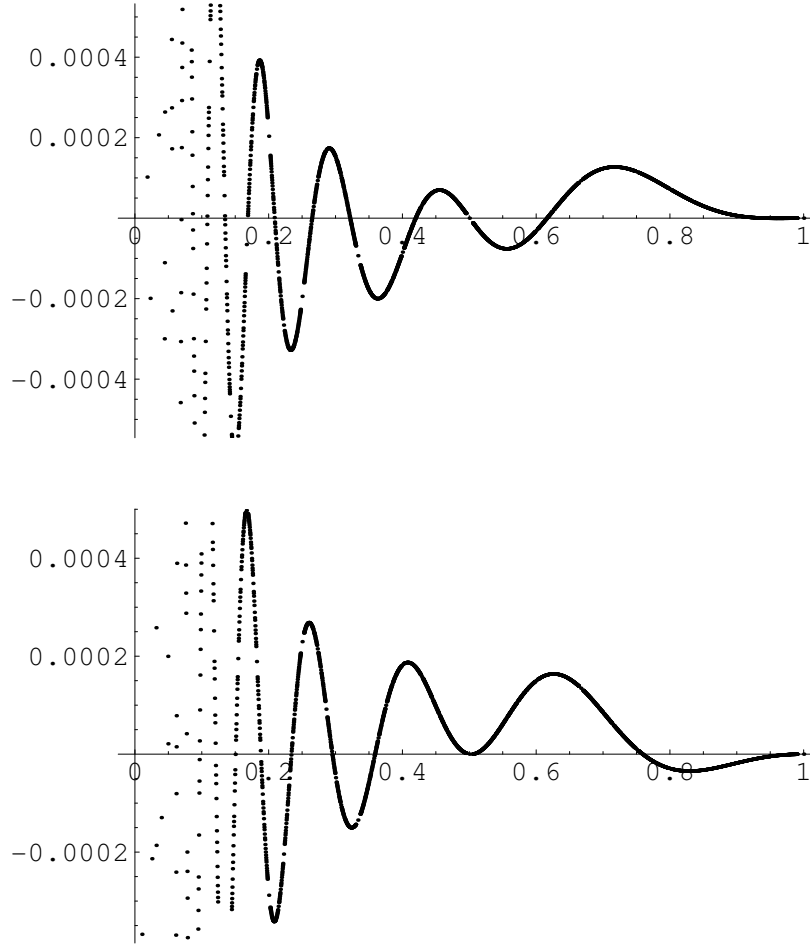


FIGURE 5. The period function ψ_{s_1} , with $\zeta(2s_1 - 1) = 0$, $2s_1 - 1 \approx \frac{1}{2} + 14.1347i$. Drawn are real (top) and imaginary (bottom) parts of $\psi_{s_1}(a/c)$ for $0 \leq \frac{a}{c} \leq 1$, $1 \leq c \leq 100$.

$$= (1 + O(\tau^{-2})) \tau^{2s} \zeta(2s, \tau) = \frac{\tau}{2s-1} + \frac{1}{2} + o(1) \quad (\tau \xrightarrow{\text{ga}} \infty).$$

This gives the meromorphic continuation to $\text{Re } s > 0$, with a first order pole at $s = \frac{1}{2}$ with residue $\frac{1}{2}\tau$ as the sole singularity in his region.

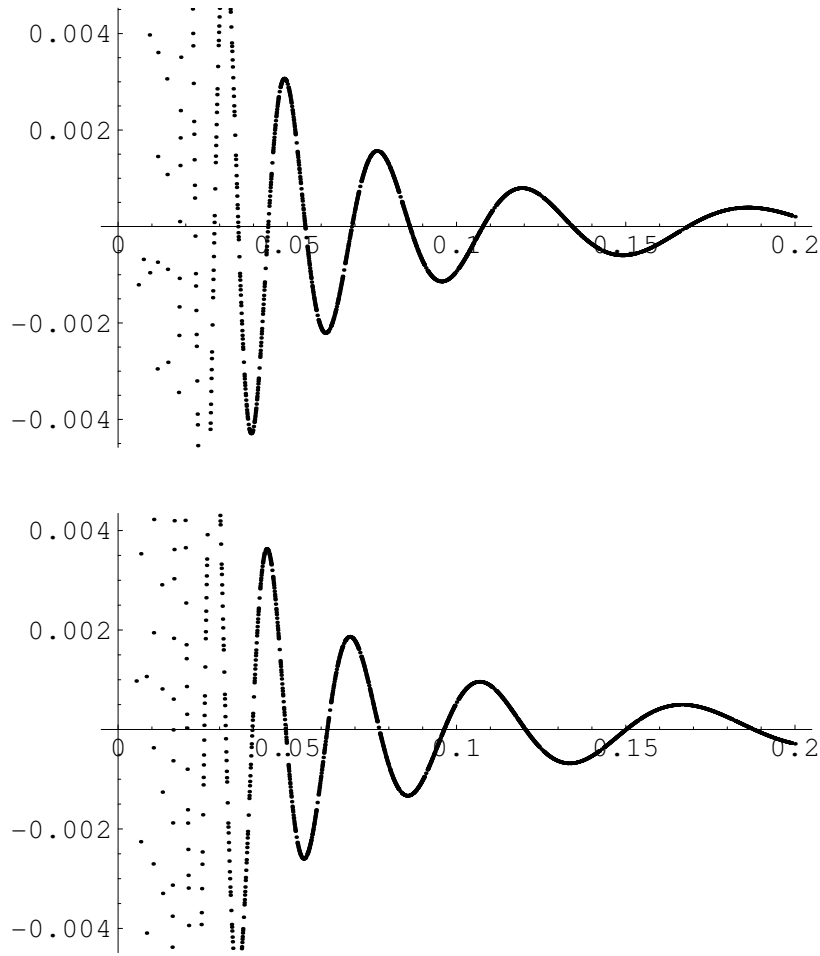


FIGURE 6. A closer look at the region near 0. Drawn are real (top) and imaginary (bottom) parts of $\psi_{s_1}(a/c)$ for $0 \leq \frac{a}{c} \leq 0.2$, $1 \leq c \leq 200$.

3'. PICTURES

Quantum Maass forms are functions on \mathbb{Q} . It is natural to look for illustrations of examples. For the Eisenstein series we have explicit formulas, that lead to illustrations easily. For the Maass cusp forms illustrations seem possible on the basis of existing numerical results. I have not spend time on that.

In all cases, we compute a function on a subset

$$\left\{ \frac{a}{c} \in [x_0, x_1] \mid a, c \in \mathbb{Z}, 0 < c \leq N \right\}$$

for some interval $[x_0, x_1] \subset \mathbb{R}$ and some rational number N .

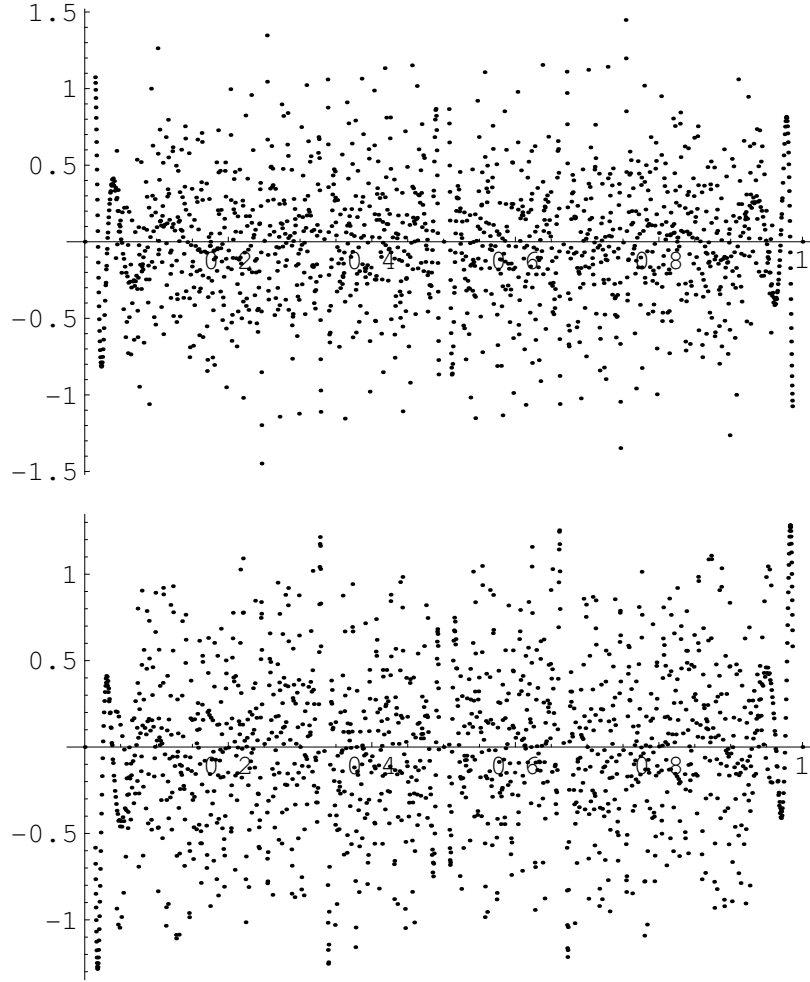


FIGURE 7. The extended quantum Maass form for the Eisenstein series E_{s_2} , with $s_2 = \frac{1}{2} + 3i$. Drawn is are the real part (top) and imaginary part (bottom) of $C_{s_2}(a/c)$ for $0 \leq \frac{a}{c} \leq 1$, $1 \leq c \leq 70$.

3.1'. **Eisenstein series.** Omitting the middle term in (16), we obtain a representative in the line model of the extended quantum Maass form associated to Eisenstein series.

$$p_s(\xi, \tau) = \frac{D_s(\xi)}{\tau - \xi} + C_s(\xi) + o(1) \quad (\tau \xrightarrow{ga} \xi), \quad (40')$$

$$D_s\left(\frac{a}{c}\right) = \frac{i}{2} c^{2s-2} \Lambda(2s-1),$$

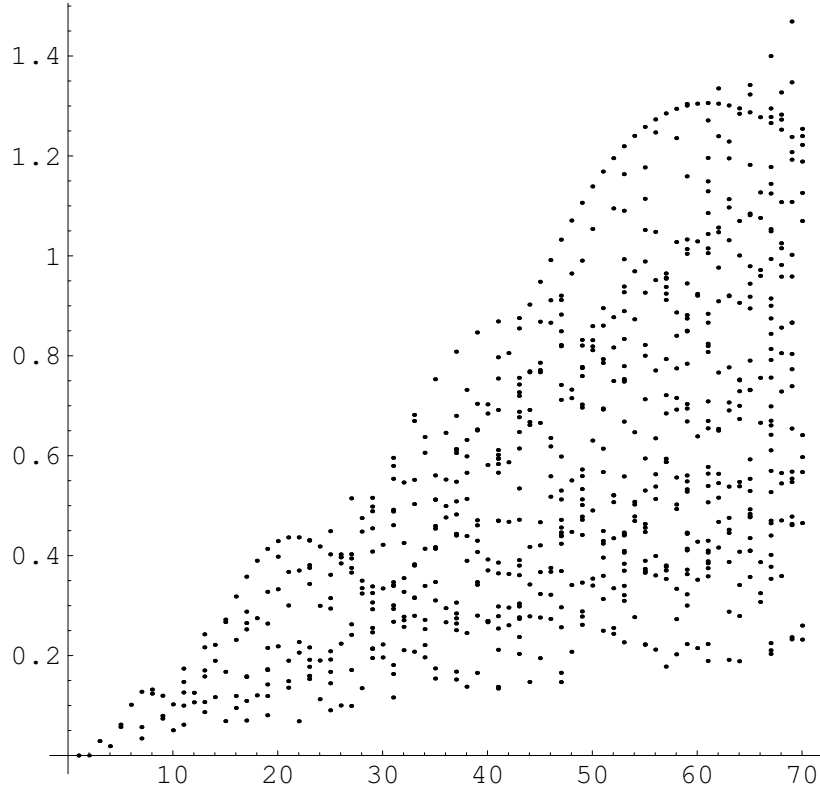


FIGURE 8. $|C_{s_2}(a/c)|$ as a function of c , for $s_2 = \frac{1}{2} + 3i$ and $1 \leq \frac{1}{c} \leq 1$, $1 \leq c \leq 70$.

$$C_s\left(\frac{a}{c}\right) = -i\pi^{\frac{1}{2}-s}\Gamma\left(s + \frac{1}{2}\right) \sum_{x=1}^{c-1} \left(\frac{dx}{c}\right) \zeta\left(2s, \frac{x}{c}\right)$$

It represents a genuine quantum Maass form if $\Lambda(2s - 1) = 0$. The first occurrence is for the first zero $z_1 \approx \frac{1}{2} + 14.5179i$ of the Riemann zeta function on the critical line. So $s_1 \approx \frac{3}{4} + 7.06736i$.

In Figure 1 the real and imaginary part of C_{s_1} are drawn by Mathematica. I have trusted the Mathematica routines for the gamma function and the Hurwitz zeta function. The graph looks rather diffuse, without clearly visible structures, except near 0 and 1. Note that we work in the line model. Hence the function is periodic. A plot of the values on C_{s_1} in the complex plane, see Figure 2, shows that the small values are more numerous. Also there is a suggestion of spiral arms. This figure also shows that $|C_{s_1}(a/c)|$ grows when the denominator c gets larger. To see how this is coupled to the argument $\frac{a}{c}$, we turn to Figure 3. The graph of $\frac{a}{c} \mapsto |C_{s_1}\left(\frac{a}{c}\right)|$ shows an avoidance of $(\xi, 0)$ if $\xi \in \mathbb{Q}$ has a small denominator. Figure 4 suggests

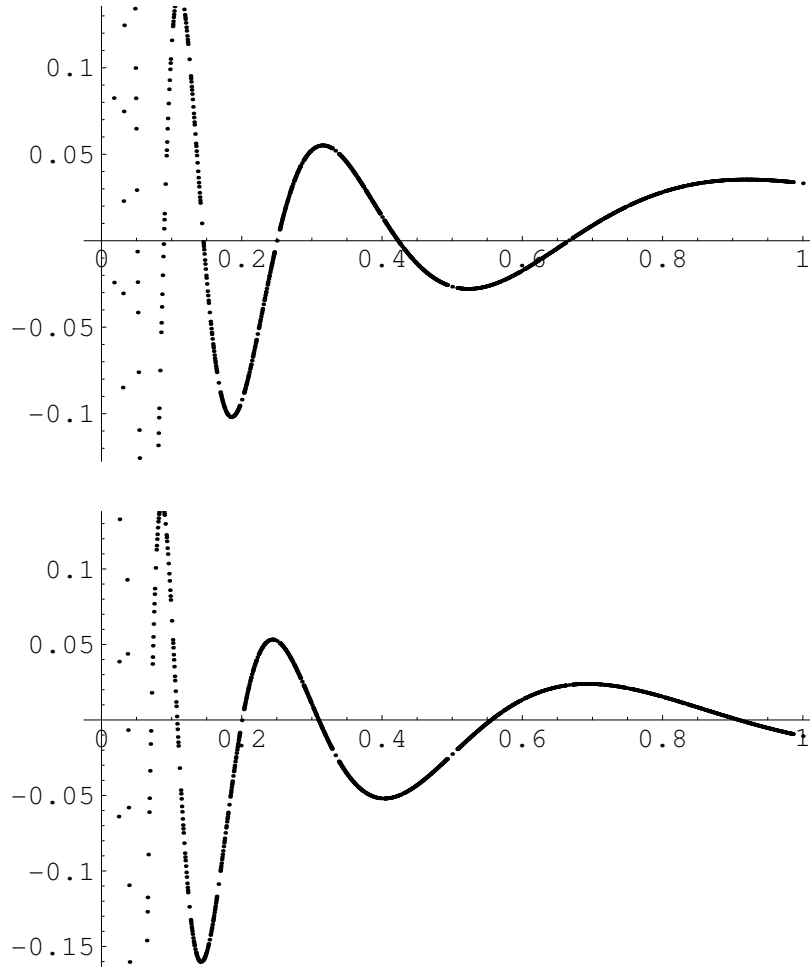


FIGURE 9. The period function for $s_2 = \frac{1}{2} + 3i$. Drawn is are the real part (top) and imaginary part (bottom) of $\psi_{s_2}(a/c)$ for $0 \leq \frac{a}{c} \leq 1$, $1 \leq c \leq 70$.

that this is not a truncation effect. This figure compares the graph of $\frac{a}{c} \mapsto \left| C_{s_1} \left(\frac{a}{c} \right) \right|$ on the region $[.3, .5] \times [0, 1.2]$ for denominators up to 40, 100, and 140. The last two graphs are equal, as far as I see. This is confirmed by Figure 2. The values of C_{s_1} move out of the window in Figure 4.

The difference $\xi \mapsto C_{s_1}(\xi) - |\xi|^{-2s_1} C_{s_1}(-1/\xi)$ should be the restriction to \mathbb{Q} of the smooth period function ψ_{s_1} . Indeed, Figure 5 shows a function that looks at least differentiable away from 0. Near 0 there seems to be a lot of oscillation. Figure 6 takes a closer look of a region near 0. I think there is more to see in these pictures. I leave that to later investigation.

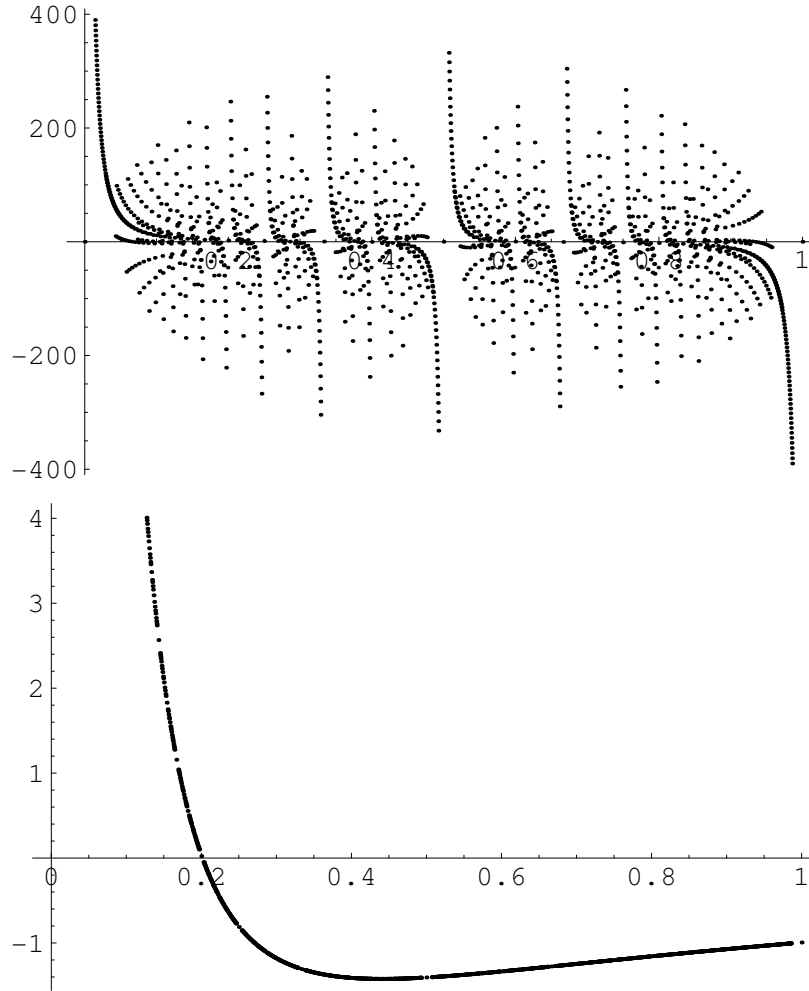


FIGURE 10. Imaginary part of $C_{.75}$ (top) and $\psi_{.75}$ (bottom) for $0 \leq \frac{a}{c} \leq 1$, $1 \leq c \leq 70$. The real parts are zero.

Let us also consider $s_2 = \frac{1}{2} + 5I$, on the critical line. Now we have an extended quantum Maass form. Figure 7 gives a picture of C_{s_2} , and Figure 8 the size of $|C_{s_2}(a/c)|$ as a function of c . In Figure 9 we see the corresponding period function. Note that the sizes are much larger than for s_1 . For all extended quantum Maass forms, the coefficient D_s is a multiple of $\frac{a}{c} \mapsto c^{2s-2}$, so there is not need to plot it.

Figure 10 treats the case $s = \frac{3}{4}$, for which C_s and ψ_s are purely imaginary. The sizes are still larger, and we see structure that asks for understanding.

3.2'. Quantum Maass forms not associated to invariant eigenfunctions. Up till now, we started with an automorphic form, an Eisenstein series, and constructed a

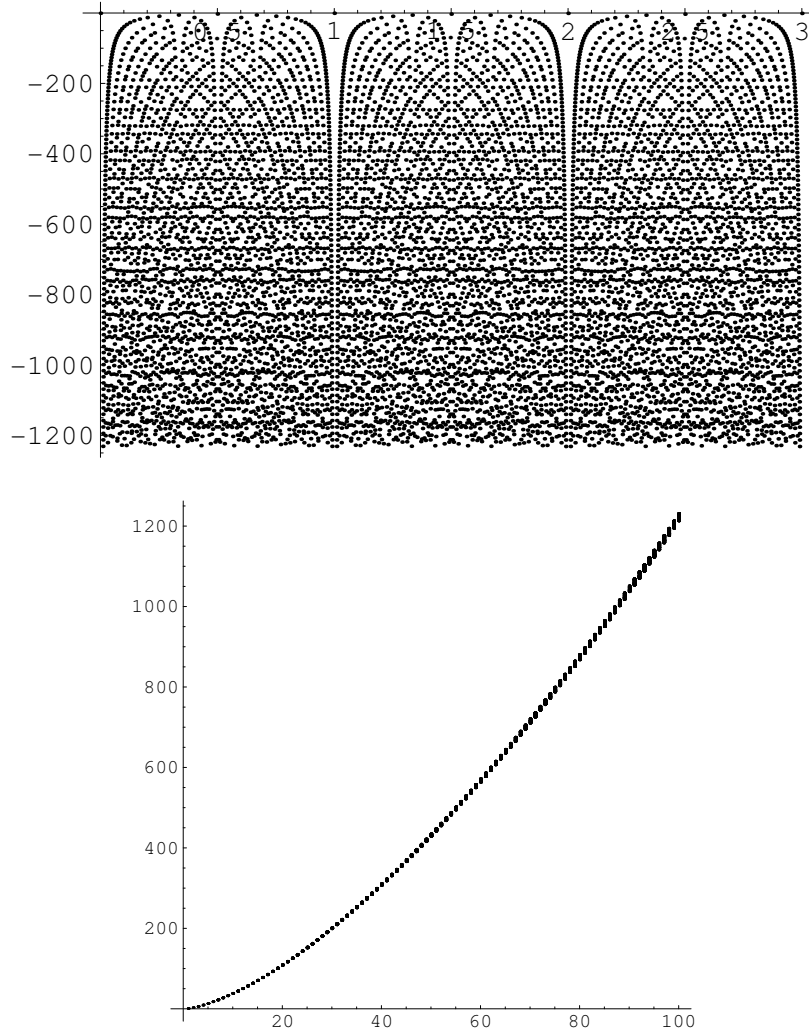


FIGURE 11. Values of a quantum Maass form C not associated to an invariant eigenfunction, see §3.2'. In the top graph is $C(a/c)$, for $s = \frac{3}{4}$, is plotted against $\frac{a}{c}$, in the bottom graph against c , for $\frac{a}{c} \in [0, 3]$, $1 \leq c \leq 100$.

quantum Maass form from it, and values of the corresponding period function. In §2.3, we start with a cocycle and construct a quantum Maass form from it.

Let us take $f^{\text{pr}} \in \mathcal{V}_s^\omega$ (projective model) given by $f(x) = \frac{x}{1+x^2}$. Since it satisfies $f^{\text{pr}}|_{2s}^{\text{pr}} S = -f^{\text{pr}}$, we can define a cocycle $c^{\text{pr}} \in Z^1(\Gamma, \mathcal{V}_s^\omega)$ by

$$c_T^{\text{pr}} = c_S^{\text{pr}} = f^{\text{pr}}. \tag{41'}$$

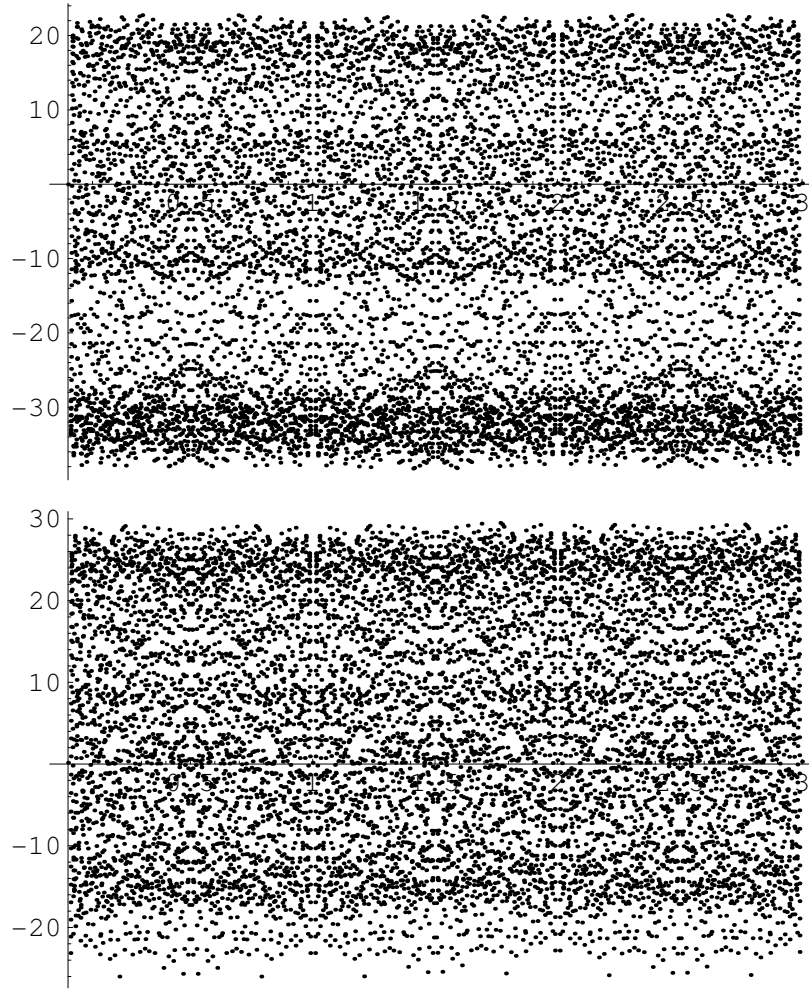


FIGURE 12. Real (top) and imaginary (bottom) part of $C(a/c)$ with $s = \frac{1}{2} + 3i$ and $0 \leq \frac{a}{c} \leq 3$, $1 \leq c \leq 100$.

In [4] we show that the cohomology class $[c^{\text{pr}}]$ is not in the image of $\mathbf{r}_s^\omega : \mathcal{E}_s^\Gamma \rightarrow H^1(\Gamma, \mathcal{V}_s^\omega)$.

From $c_T^{\text{pr}}(\infty) = 0$ it follows that the construction in the proof of Theorem 4 yields a genuine quantum Maass form, represented by $p^{\text{pr}} \in \mathcal{R}_s$ that satisfies $p^{\text{pr}}(\infty, \tau) = -c_T^{\text{pr}}|_{2s} \mathbf{A}v_T^+(\tau) = o(1)$ ($\tau \xrightarrow{\text{ga}} \infty$).

$$\begin{aligned}
 p^{\text{pr}}(\infty, \tau) &= - \sum_{n=0}^{\infty} \left(\frac{1 + \tau^2}{1 + (\tau + n)^2} \right)^s \frac{\tau + n}{1 + (\tau + n)^2} + o(1) \\
 &= -\tau^{2s} \left(1 + O(\tau^{-2}) \right) \sum_{n=0}^{\infty} (\tau + n) \left(1 + (\tau + n)^2 \right)^{-s-1} + o(1)
 \end{aligned} \tag{42'}$$

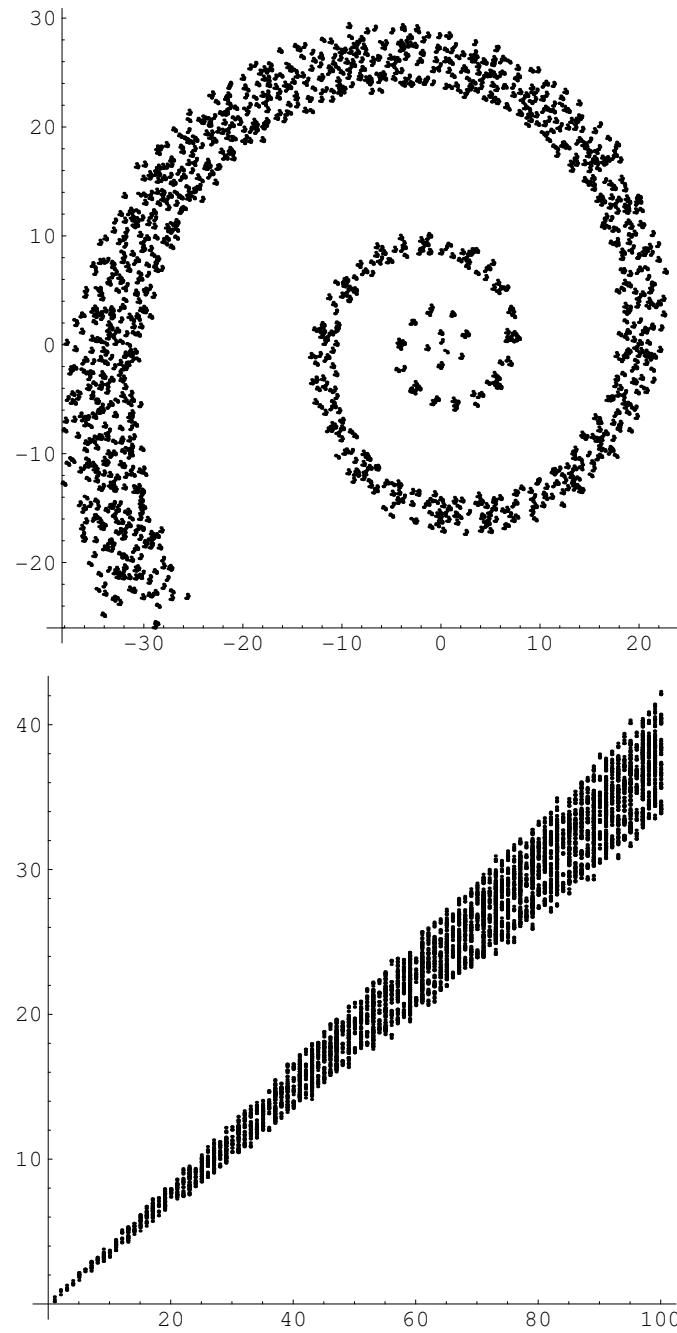


FIGURE 13. For $s = \frac{1}{2} + 3i$ and $0 \leq \frac{a}{c} \leq 3$, $1 \leq c \leq 100$, the top graph gives the values of $C(a/c)$ plotted in the complex plane, and the bottom graph gives $|C(a/c)|$ against c .

$$\begin{aligned}
&= -\tau^{2s} \left(1 + O\left(\tau^{-2}\right)\right) \left(\zeta(2s+1, \tau) + O_s\left(|\tau|^{-2\operatorname{Re} s-2}\right)\right) + o(1) \\
&= -\frac{1}{2s} + o(1).
\end{aligned}$$

So $p^{\operatorname{pr}}(\xi, \tau) = p^{\operatorname{pr}}(\xi)$, and $p^{\operatorname{pr}}(0) = p^{\operatorname{pr}}(\infty) + c_s^{\operatorname{pr}}(\infty) = -\frac{1}{2s} + 0$.

Going over to the line model: $C(x) = \left(1 + \xi^2\right)^{-s} p^{\operatorname{pr}}(\xi)$, we have

$$\begin{aligned}
C(0) &= -\frac{1}{2s}, & (43') \\
C(\xi) &= C(\xi+1) + \xi \left(1 + \xi^2\right)^{-s-1} & \text{for } \xi \in \mathbb{Q}, \\
C(\xi) &= |\xi|^{-2s} C(-1/\xi) + \xi \left(1 + \xi^2\right)^{-s-1} & \text{for } \xi \in \mathbb{Q} \setminus \{0\}.
\end{aligned}$$

This can be used for recursive computation of C .

Figure 11 gives results for $s = \frac{3}{4}$. The graph looks periodic. It is not, but the values of $f = c_T$ are small in comparison with those of C . We see also that $C(a/c)$ is almost completely determined by c .

For $s = \frac{1}{2} + 3i$, the graphs in Figure 12 look more chaotic. In Figure 13 we see that the size of $C(a/c)$ is strongly related to c .

Utrecht, April 2006 (and a few changes February 2007)

Roelof Bruggeman